

The origin of the 95 GeV excess in the flavor-dependent $U(1)_X$ model

Zhao-feng Ge^{1,2*}, Feng-Yan Niu^{3,4,5}, Jin-Lei Yang^{3,4,5†}

¹*CAS Key Laboratory of Theoretical Physics, Institute of Theoretical Physics, Chinese Academy of Sciences, Beijing 100190, China*

²*School of Physical Sciences, University of Chinese Academy of Sciences, Beijing 100049, China and*

³*Department of Physics, Hebei University, Baoding, 071002, China*

⁴*Key Laboratory of High-precision Computation and Application of Quantum Field Theory of Hebei Province, Baoding, 071002, China*

⁵*Research Center for Computational Physics of Hebei Province, Baoding, 071002, China*

Abstract

This study investigates the excesses observed in the CMS diphoton and ditau data around 95 GeV within the framework of the flavor-dependent $U(1)_X$ model. The model introduces a singlet scalar to explain the nonzero neutrino masses. This newly introduced Higgs interacts directly with the quark sector, motivated by the aim to explain the flavor numbers of the fermion sector. Additionally, it undergoes mixing with the SM-like Higgs boson. The study suggests that designating this singlet Higgs state in this model as the lightest Higgs boson holds great potential for explaining the excesses around 95 GeV. In the calculations, we maintained the masses of the lightest and next-to-lightest Higgs bosons at around 95 GeV and 125 GeV respectively. It was found that the theoretical predictions on the signal strengths $\mu(h_{95})_{\gamma\gamma}$, $\mu(h_{95})_{\tau\tau}$ in the flavor-dependent $U(1)_X$ model can be fitted well to the excesses observed at CMS.

Keywords: 95 GeV excesses, $U(1)_X$ model, new Higgs states

* gezhaofeng@itp.ac.cn

† jlyang@hbu.edu.cn

I. INTRODUCTION

The discovery of a 125 GeV Higgs boson at the Large Hadron Collider (LHC) in 2012 [1, 2] stands as one of the most remarkable achievements in theoretical physics. Its properties align well with the predictions of the standard model (SM) [3, 4], suggesting the observation of all fundamental particles anticipated by the SM.

The current focus of the LHC program is to determine whether the detected Higgs boson is the sole fundamental scalar particle or part of a new physics (NP) theory with an extended Higgs sector. As of now, no new scalars have been discovered at the LHC. However, there have been several intriguing excesses observed in searches for light Higgs bosons below 125 GeV, accompanied by increasing precision in the measurements of the Higgs couplings to fermions and gauge bosons.

The results derived from both the CMS Run 1 and the first year of CMS Run 2 data for Higgs-boson searches in the diphoton final state show a 2.8σ local excess at a mass about 95 GeV [5, 6], which is compatible with the latest ATLAS result [7] based on the previously reported result utilizing 80 fb^{-1} [8] in the diphoton searches

$$\mu(\Phi_{95})_{\gamma\gamma} = \frac{\sigma(gg \rightarrow \Phi_{95}^{\text{NP}})\text{BR}(\Phi_{95}^{\text{NP}} \rightarrow \gamma\gamma)}{\sigma(gg \rightarrow h_{95}^{\text{SM}})\text{BR}(h_{95}^{\text{SM}} \rightarrow \gamma\gamma)} = 0.18 \pm 0.10. \quad (1)$$

Utilizing the full Run 2 dataset, CMS published the results for the Higgs boson searches in the $\tau^+\tau^-$ channel, indicating a local significance of 3.1σ at a mass value around 95 GeV [9]

$$\mu(\Phi_{95})_{\tau\tau} = \frac{\sigma(gg \rightarrow \Phi_{95}^{\text{NP}})\text{BR}(\Phi_{95}^{\text{NP}} \rightarrow \tau\tau)}{\sigma(gg \rightarrow h_{95}^{\text{SM}})\text{BR}(h_{95}^{\text{SM}} \rightarrow \tau\tau)} = 1.2 \pm 0.5. \quad (2)$$

Recently, a new analysis of Higgs-boson searches in the diphoton final state by CMS has further confirmed the excess at approximately 95 GeV. The results are reported in [10].

$$\mu(\Phi_{95})_{\gamma\gamma} = 0.33_{-0.12}^{+0.19}. \quad (3)$$

Theoretically, there are numerous discussions on the excesses in NP models. The analysis carried out in Refs. [11–25] indicates that the diphoton rate may be several times larger than its SM prediction for the same scalar mass in the next-to-minimal supersymmetric standard model (NMSSM). In the Two-Higgs doublet model (2HDM) with an additional real singlet

(N2HDM), the possibilities of explaining the observed excesses are studied in Refs. [26–34]. The authors of Ref. [35] explore the viability of the radion mixed Higgs to be the 125 GeV boson along with the presence of a light radion which can account for the CMS diphoton excess well in the Higgs-radion mixing model. Considering the one-loop corrections to the neutral scalar masses of the $\mu\nu$ SSM, the authors of Refs. [36, 37] demonstrate how the $\mu\nu$ SSM can simultaneously accommodate two excesses measured at the Large Electron-Positron [38] and LHC at the 1σ level. Based on the analysis in Ref. [39], extending the scalar sector with a $SU(2)_L$ triplet with hypercharge $Y = 0$ can well provide the origin of the 95 GeV excesses. Whether certain model realizations could simultaneously explain the two excesses while being in agreement with all other Higgs-boson related limits and measurements were reviewed in Refs. [40, 41].

In the flavor-dependent $U(1)_X$ model, the new $U(1)_X$ charge is related to the baryon and lepton number, and the origin of the number of observed fermion families can be well explained by imposing a relation involved by the color number 3 [42]. Because of the Z_2 conservation, the model can contain several scenarios for single-component dark matter. In addition, the nonzero neutrino masses can be obtained elegantly by type-I see-saw mechanism by the new introduced singlet scalar and the nonzero $U(1)_X$ charges of neutrinos. As a result, the new introduced CP-even scalar may be assigned to account for the excesses at about 95 GeV. Based on the characters of the new introduced CP-even scalar in the flavor-dependent $U(1)_X$ model, we focus on investigating the diphoton and ditau excesses at about 95 GeV in this work¹.

The paper is organized as follows. The scalar sector and fermion masses terms of the flavor-dependent $U(1)_X$ model are given in Sec. II. The numerical results are present and analyzed in Sec. III. Finally, a summary is made in Sec. IV.

¹ As analyzed in Refs. [43, 44], the light CP-even Higgs does suffers strict constraints from the LHC search for the top-quark associated production of the SM Higgs boson that decays into $\tau\bar{\tau}$, and the possibility to explain the ditau excess by the CP-even scalar is excluded according the analysis in Ref. [44]. However, they consider the 1σ range of $\mu(\Phi_{95})_{\tau\tau}$ in the analysis, it is found that this constraint can be relaxed if the 2σ range of $\mu(\Phi_{95})_{\tau\tau}$ is considered. And the coupling properties of 125 GeV Higgs in the flavor-dependent $U(1)_X$ model are different from the ones of 125 GeV Higgs in the SM, so the 125 GeV signal strength constraints are also taken into account in the analysis.

II. THE $U(1)_X$ MODEL AND ITS HIGGS SECTOR

The flavor-dependent $U(1)_X$ model [42] is one of the simplest extension of the SM that introduces a flavor-dependent additional gauge group $U(1)_X$. The gauge group of the model is $SU(3)_C \otimes SU(2)_L \otimes U(1)_Y \otimes U(1)_X$ in the model, and local $U(1)_X$ gauge group is not family universal. The new charge X , combines lepton (L) and baryon (B) numbers, are defined as

$$X = xB + yL, \quad (4)$$

and X depends on family. For each flavor i , $X = x_i b + y_i L$, where x_i and y_i are functions of i for $i = 1, 2, \dots, N_f$, while B and L denotes the total baryon or lepton numbers, respectively.

The SM fermions transform under the gauge symmetry as

$$\begin{aligned} l_{iL} &= \begin{pmatrix} \nu_{iL} \\ e_{iL} \end{pmatrix} \sim (1, 2, -1/2, y_i), \quad q_{iL} = \begin{pmatrix} u_{iL} \\ d_{iL} \end{pmatrix} \sim (3, 2, 1/6, x_i/3), \\ e_{iR} &\sim (1, 1, -1, y_i), \quad u_{iR} \sim (3, 1, 2/3, x_i/3), \quad d_{iR} \sim (3, 1, -1/3, x_i/3), \end{aligned} \quad (5)$$

where x_i are family dependent, and y_i do not. The charges of all fields in this model are presented in Table I, where $a = 1, 2, 3$, $\alpha = 1, 2$, and z is arbitrarily nonzero.

This model can explain the origin of the observed number of fermion families and potentially offer solutions for both neutrino mass and dark matter, which differs from the traditional $U(1)_{B-L}$ extension. The total scalar potential in this model is given by [42]

$$\begin{aligned} V &= \mu_1^2 \Phi^\dagger \Phi + \mu_2^2 \chi^* \chi + \mu_3^2 \eta^* \eta + \lambda_1 (\Phi^\dagger \Phi)^2 + \lambda_2 (\chi^* \chi)^2 + \lambda_3 (\eta^* \eta)^2 + \\ &\lambda_4 (\Phi^\dagger \Phi)(\chi^* \chi) + \lambda_5 (\Phi^\dagger \Phi)(\eta^* \eta) + \lambda_6 (\chi^* \chi)(\eta^* \eta) \end{aligned} \quad (6)$$

where λ 's are dimensionless, and μ 's have mass dimension. To ensure the stability of the scalar potential, the free parameters $\lambda_1, \lambda_2, \lambda_3, \mu_1, \mu_2, \mu_3$ should satisfy

$$\lambda_{1,2,3} > 0, \quad \mu_{1,2}^2 < 0, \quad \mu_3^2 > 0. \quad (7)$$

The local gauge symmetry $SU(2)_L \otimes U(1)_Y \otimes U(1)_X$ breaks down to the electromagnetic symmetry $U(1)_{\text{em}}$ as the scalar fields receive nonzero vacuum expectation values (VEV):

$$\Phi = \begin{pmatrix} \Phi_1^+ \\ \frac{1}{\sqrt{2}}(v + S_1 + iA_1) \end{pmatrix}, \quad \chi = \frac{1}{\sqrt{2}}(\Lambda + S_2 + iA_2), \quad \eta = \frac{1}{\sqrt{2}}(S_3 + iA_3). \quad (8)$$

Multiplets	$SU(3)_C$	$SU(2)_L$	$U(1)_Y$	$U(1)_X$	Z_2
$l_{aL} = (\nu_{aL}, e_{aL})^T$	1	2	$-\frac{1}{2}$	z	+
ν_{aR}	1	1	0	z	+
e_{aR}	1	1	-1	z	+
$q_{\alpha L} = (u_{\alpha L}, d_{\alpha L})^T$	3	2	$\frac{1}{6}$	z	+
$u_{\alpha R}$	3	1	$\frac{2}{3}$	-z	+
$d_{\alpha R}$	3	1	$-\frac{1}{3}$	-z	+
$q_{3L} = (u_{3L}, d_{3L})^T$	3	2	$\frac{1}{6}$	z	+
u_{3R}	3	1	$\frac{2}{3}$	z	+
d_{3R}	3	1	$-\frac{1}{3}$	z	+
$\Phi = (\Phi_1^+, \Phi_2^0)^T$	1	2	$\frac{1}{2}$	0	+
χ	1	1	0	-2z	+
ξ	1	1	0	2z	-
η	1	1	0	z	-

TABLE I: Multiplets in the flavor-dependent $U(1)_X$ model [42].

Substituting them into the scalar potential Eq. (6), the tadpole equations give

$$\mu_1^2 = -\frac{1}{2}(2\lambda_1 v^2 + \lambda_4 \Lambda^2), \quad \mu_2^2 = -\frac{1}{2}(2\lambda_2 \Lambda^2 + \lambda_4 v^2). \quad (9)$$

Due to Z_2 conservation, the dark scalars S_3 and A_3 do not mix with the other scalars and are degenerate in mass. On the basis (S_1, S_2, S_3) , the squared mass matrix of Higgs can be written as

$$M_h^2 = \begin{pmatrix} 2\lambda_1 v^2 & \lambda_4 v \Lambda & 0 \\ \lambda_4 v \Lambda & 2\lambda_2 \Lambda^2 & 0 \\ 0 & 0 & \frac{1}{2}(\lambda_5 v^2 + \lambda_6 \Lambda^2 + 2\mu_3^2) \end{pmatrix}, \quad (10)$$

where S_1 and S_2 are mixed by the term $\lambda_4 v \Lambda$. The squared mass matrix M_h^2 in Eq. (10) can be diagonalized by the unitary matrix Z_h as

$$\text{diag}(m_{h_1}^2, m_{h_2}^2, m_{h_3}^2) = Z_h \cdot M_h^2 \cdot Z_h^\dagger, \quad (11)$$

where $m_{h_1}, m_{h_2}, m_{h_3}$ are the physical Higgs masses. And under the assumption $v/\Lambda \ll 1$, $\lambda_2 \ll 1$ and $\lambda_4 \ll 1$, we can obtain

$$m_{h_1}^2 \approx 2\lambda_2\Lambda^2 + \frac{\lambda_4^2}{2\lambda_2}v^2, \quad m_{h_2}^2 \approx 2\lambda_1v^2, \quad m_{h_3}^2 = \frac{1}{2}(\lambda_5v^2 + \lambda_6\Lambda^2 + 2\mu_3^2). \quad (12)$$

Z_h can be parameterized as

$$Z_h = \begin{pmatrix} -\sin\theta & \cos\theta & 0 \\ \cos\theta & \sin\theta & 0 \\ 0 & 0 & 1 \end{pmatrix}, \quad (13)$$

where the mixing angle $\cos^2\theta = \frac{1}{2}(\frac{1}{\sqrt{1+A^2}} + 1)$ with $A = -\frac{\lambda_4 v \Lambda}{\lambda_1 v^2 - \lambda_2 \Lambda^2}$.

After spontaneous symmetry breaking, the fermion mass terms are given by the Yukawa couplings

$$\begin{aligned} \mathcal{L} \sim & h_{ab}^e \bar{l}_{aL} \Phi e_{bR} + h_{ab}^v \bar{l}_{aL} \tilde{\Phi} \nu_{bR} + \frac{1}{2} f_{ab}^\nu \bar{\nu}_{aR}^c \nu_{bR} \chi + h_{\alpha\beta}^d \bar{q}_{\alpha L} \Phi d_{\beta R} + h_{\alpha\beta}^u \bar{q}_{\alpha L} \tilde{\Phi} u_{\beta R} \\ & + h_{33}^d \bar{q}_{3L} \Phi d_{3R} + h_{33}^u \bar{q}_{3L} \tilde{\Phi} u_{3R} + \frac{h_{\alpha 3}^d}{M} \bar{q}_{\alpha L} \Phi \chi d_{3R} + \frac{h_{3\alpha}^u}{M} \bar{q}_{3L} \tilde{\Phi} \chi^* u_{\alpha R} \\ & + \frac{h_{3\alpha}^d}{M} \bar{q}_{3L} \Phi \chi^* d_{\alpha R} + \frac{h_{\alpha 3}^u}{M} \bar{q}_{\alpha L} \tilde{\Phi} \chi u_{3R} + y_\alpha \bar{\xi}_L \eta \nu_{\alpha R} - m_\xi \bar{\xi}_L \xi_R + h.c., \end{aligned} \quad (14)$$

where $a, b = 1, 2, 3$, $\alpha, \beta = 1, 2$. The fermion-antifermion-higgs couplings on the interactional basis can be written as

$$\begin{aligned} \mathcal{L} \sim & \frac{1}{\sqrt{2}} h_{ab}^e \bar{e}_{aL} S_1 e_{bR} + \frac{1}{\sqrt{2}} h_{ab}^v \bar{\nu}_{aL} S_1 \nu_{bR} + \frac{1}{\sqrt{2}} h_{\alpha\beta}^d \bar{d}_{\alpha L} S_1 d_{\beta R} + \\ & \frac{1}{\sqrt{2}} h_{\alpha\beta}^u \bar{u}_{\alpha L} S_1 u_{\beta R} + \frac{1}{\sqrt{2}} h_{33}^d \bar{d}_{3L} S_1 d_{3R} + \frac{1}{\sqrt{2}} h_{33}^u \bar{u}_{3L} S_1 u_{3R} + \\ & \frac{h_{\alpha 3}^d}{2M} (v \bar{d}_{\alpha L} S_2 d_{3R} + \Lambda \bar{d}_{\alpha L} S_1 d_{3R}) + \frac{h_{3\alpha}^u}{2M} (v \bar{u}_{3L} S_2 u_{\alpha R} + \Lambda \bar{u}_{3L} S_1 u_{\alpha R}) + \\ & \frac{h_{3\alpha}^d}{2M} (v \bar{d}_{3L} S_2 d_{\alpha R} + \Lambda \bar{d}_{3L} S_1 d_{\alpha R}) + \frac{h_{\alpha 3}^u}{2M} (v \bar{u}_{\alpha L} S_2 u_{3R} + \Lambda \bar{u}_{\alpha L} S_1 u_{3R}). \end{aligned} \quad (15)$$

It is worth noting the presence of additional terms compared to the quark mass matrices in the SM, such as $\frac{h_{\alpha 3}^d}{2M} (v \bar{d}_{3L} S_2 d_{\alpha R} + \Lambda \bar{d}_{3L} S_1 d_{\alpha R})$ in the down-quark sector, $\frac{h_{3\alpha}^u}{2M} (v \bar{u}_{3L} S_2 u_{\alpha R} + \Lambda \bar{u}_{3L} S_1 u_{\alpha R})$ in the up-quark sector and etc. Under the minimal flavor violation assumption [45–49] which can release the model from the experimental constraints on the processes

mediated by flavor-changing neutral currents (FCNCs), the fermion-antifermion-higgs couplings on the physical basis $h_1 \bar{f}_i^m f_i^m$, ($q = u, d, e$) can be written as

$$\begin{aligned}
\mathcal{L}_{\mathcal{I}} = & h_1 (\bar{d}_1^m, \bar{d}_2^m, \bar{d}_3^m) \begin{pmatrix} m_d/v & 0 & 0 \\ 0 & m_s/v & 0 \\ 0 & 0 & m_b/v \end{pmatrix} \begin{pmatrix} d_1^m \\ d_2^m \\ d_3^m \end{pmatrix} (Z_{11}^h + Z_{21}^h \kappa_1) + \\
& h_1 (\bar{u}_1^m, \bar{u}_2^m, \bar{u}_3^m) \begin{pmatrix} m_u/v & 0 & 0 \\ 0 & m_c/v & 0 \\ 0 & 0 & m_t/v \end{pmatrix} \begin{pmatrix} u_1^m \\ u_2^m \\ u_3^m \end{pmatrix} (Z_{11}^h + Z_{21}^h \kappa_2) + \\
& h_1 (\bar{e}_1^m, \bar{e}_2^m, \bar{e}_3^m) \begin{pmatrix} m_e/v & 0 & 0 \\ 0 & m_\mu/v & 0 \\ 0 & 0 & m_\tau/v \end{pmatrix} \begin{pmatrix} e_1^m \\ e_2^m \\ e_3^m \end{pmatrix} (Z_{11}^h). \tag{16}
\end{aligned}$$

Here, the contributions from the additional terms in the quark sector are absorbed into the constants κ_1 and κ_2 with

$$\begin{aligned}
\kappa_1 m_{d_i} = & \left[Z_L^{d\dagger} \begin{pmatrix} 0 & 0 & -h_{13}^d \frac{v\Lambda}{2M} \\ 0 & 0 & -h_{23}^d \frac{v\Lambda}{2M} \\ -h_{31}^d \frac{v\Lambda}{2M} & -h_{32}^d \frac{v\Lambda}{2M} & 0 \end{pmatrix} Z_R^d \right] (i, i), \\
\kappa_2 m_{u_i} = & \left[Z_L^{u\dagger} \begin{pmatrix} 0 & 0 & -h_{13}^u \frac{v\Lambda}{2M} \\ 0 & 0 & -h_{23}^u \frac{v\Lambda}{2M} \\ -h_{31}^u \frac{v\Lambda}{2M} & -h_{32}^u \frac{v\Lambda}{2M} & 0 \end{pmatrix} Z_R^u \right] (i, i), \tag{17}
\end{aligned}$$

where m_{q_i} denotes the i -th quark q mass, Z_L^q and Z_R^q are the unitary matrices which diagonalize the mass matrix of quark q , and (i, i) denotes the i -th diagonal element of matrix. It is obvious that κ_1 , κ_2 depend on the parameters Λ , M and the Yukawa coupling constant complicatedly. For simplicity, as shown in Eq. (16), we take the diagonal elements of the matrices defined as $\kappa_1 m_{d_i}$, $\kappa_2 m_{u_i}$ as inputs to carry out the analysis.

As defined in the introduction sector, the diphoton and ditau signal strength are

$$\begin{aligned}\mu(h_{95})_{\gamma\gamma} &= \frac{\sigma(gg \rightarrow h_{95}^{\text{NP}})\text{BR}(h_{95}^{\text{NP}} \rightarrow \gamma\gamma)}{\sigma(gg \rightarrow h_{95}^{\text{SM}})\text{BR}(h_{95}^{\text{SM}} \rightarrow \gamma\gamma)}, \\ \mu(h_{95})_{\tau\tau} &= \frac{\sigma(gg \rightarrow h_{95}^{\text{NP}})\text{BR}(h_{95}^{\text{NP}} \rightarrow \tau\tau)}{\sigma(gg \rightarrow h_{95}^{\text{SM}})\text{BR}(h_{95}^{\text{SM}} \rightarrow \tau\tau)},\end{aligned}\quad (18)$$

where [50]

$$\begin{aligned}\Gamma_{\text{tot},95}^{\text{SM}} &\approx 0.00259 \text{ GeV}, \\ \text{BR}(h_{95}^{\text{SM}} \rightarrow \gamma\gamma) &\approx 1.4 \times 10^{-3}, \quad \text{BR}(h_{95}^{\text{SM}} \rightarrow \tau\tau) \approx 0.082,\end{aligned}\quad (19)$$

and the top quark loop is considered in calculating the production cross section of the 95 GeV Higgs at the LHC for simplicity. The contributions from NP can be written as [24]

$$\begin{aligned}\Gamma_{\text{tot},95}^{\text{NP}} &\approx C_{h_{95}dd}^2 \Gamma_{bb,95}^{\text{SM}} + C_{h_{95}ee}^2 \Gamma_{\tau\bar{\tau},95}^{\text{SM}} + C_{h_{95}uu}^2 (\Gamma_{c\bar{c},95}^{\text{SM}} + \Gamma_{gg,95}^{\text{SM}}) \\ \text{BR}(h_{95}^{\text{NP}} \rightarrow \gamma\gamma) &\approx C_{h_{95}uu}^2 \text{BR}(h_{95}^{\text{SM}} \rightarrow \gamma\gamma) \frac{\Gamma_{\text{tot},95}^{\text{SM}}}{\Gamma_{\text{tot},95}^{\text{NP}}}, \\ \text{BR}(h_{95}^{\text{NP}} \rightarrow \tau\bar{\tau}) &\approx C_{h_{95}ee}^2 \text{BR}(h_{95}^{\text{SM}} \rightarrow \tau\bar{\tau}) \frac{\Gamma_{\text{tot},95}^{\text{SM}}}{\Gamma_{\text{tot},95}^{\text{NP}}},\end{aligned}\quad (20)$$

where the coefficients $C_{h_{95}uu}$, $C_{h_{95}dd}$, $C_{h_{95}ee}$ are the normalized couplings of 95 GeV Higgs in NP models with SM particles (in units of the corresponding SM couplings). In the conventional $U(1)_X$ model, we have

$$\begin{aligned}C_{h_{95}uu} &= C_{h_{1uu}} = Z_{h,11} + Z_{h,21}\kappa_1, \quad C_{h_{95}dd} = C_{h_{1dd}} = Z_{h,11} + Z_{h,21}\kappa_2, \\ C_{h_{95}ee} &= C_{h_{1dd}} = Z_{h,11}.\end{aligned}\quad (21)$$

As shown above, the extra scalar singlet (which is designed to be the 95 GeV scalar state) couples to the SM quarks at the tree level, and the corresponding effects are collected to the newly defined parameters κ_1, κ_2 . Hence, there are two sources to accommodate the excesses in the diphoton and ditau channels in the model. The first one comes from the tree level couplings between the extra scalar singlet with the SM quarks, and the second one comes from the mixing of the 95 GeV scalar state with the 125 GeV one. It indicates that the 125 GeV Higgs boson signal strength measurements should be considered in the analysis.

Generally, the signal strengths for the 125 GeV Higgs decay channels can be quantified as [51]

$$\begin{aligned}\mu(h_{125})_{\gamma\gamma, VV^*}^{\text{ggF}} &= \frac{\sigma(gg \rightarrow h_{125}^{\text{NP}})\text{BR}(h_{125}^{\text{NP}} \rightarrow \gamma\gamma, VV^*)}{\sigma(gg \rightarrow h_{125}^{\text{SM}})\text{BR}(h_{125}^{\text{SM}} \rightarrow \gamma\gamma, VV^*)}, (V = W, Z) \\ \mu(h_{125})_{ff}^{\text{VBF}} &= \frac{\sigma(VV^* \rightarrow h_{125}^{\text{NP}})\text{BR}(h_{125}^{\text{NP}} \rightarrow f\bar{f})}{\sigma(VV^* \rightarrow h_{125}^{\text{SM}})\text{BR}(h_{125}^{\text{SM}} \rightarrow f\bar{f})}, (f = b, \tau, c),\end{aligned}\quad (22)$$

where ggF and VBF stand for gluon-gluon fusion and vector boson fusion respectively. The corresponding SM decay width and fractions can be found in ref [52]. The contributions from NP can be written as

$$\begin{aligned}\Gamma_{\text{tot},125}^{\text{NP}} &\approx C_{h_{125}dd}^2 \Gamma_{bb,125}^{\text{SM}} + C_{h_{125}uu}^2 \Gamma_{c\bar{c},125}^{\text{SM}} + C_{h_{125}ee}^2 \Gamma_{\tau\bar{\tau},125}^{\text{SM}} + C_{h_{125}VV}^2 (\Gamma_{WW^*,125}^{\text{SM}} + \Gamma_{ZZ^*,125}^{\text{SM}}), \\ \text{BR}(h_{125}^{\text{NP}} \rightarrow \gamma\gamma) &\approx C_{h_{125}uu}^2 \text{BR}(h_{125}^{\text{SM}} \rightarrow \gamma\gamma) \frac{\Gamma_{\text{tot},125}^{\text{SM}}}{\Gamma_{\text{tot},125}^{\text{NP}}}, \\ \text{BR}(h_{125}^{\text{NP}} \rightarrow \tau\bar{\tau}) &\approx C_{h_{125}ee}^2 \text{BR}(h_{125}^{\text{SM}} \rightarrow \tau\bar{\tau}) \frac{\Gamma_{\text{tot},125}^{\text{SM}}}{\Gamma_{\text{tot},125}^{\text{NP}}}, \\ \text{BR}(h_{125}^{\text{NP}} \rightarrow b\bar{b}) &\approx C_{h_{125}dd}^2 \text{BR}(h_{125}^{\text{SM}} \rightarrow \tau\bar{\tau}) \frac{\Gamma_{\text{tot},125}^{\text{SM}}}{\Gamma_{\text{tot},125}^{\text{NP}}}, \\ \text{BR}(h_{125}^{\text{NP}} \rightarrow VV^*) &\approx C_{h_{125}VV}^2 \text{BR}(h_{125}^{\text{SM}} \rightarrow \tau\bar{\tau}) \frac{\Gamma_{\text{tot},125}^{\text{SM}}}{\Gamma_{\text{tot},125}^{\text{NP}}},\end{aligned}\quad (23)$$

where the coefficients $C_{h_{125}uu}$, $C_{h_{125}dd}$, $C_{h_{125}ee}$ and $C_{h_{125}VV}$ are the normalized couplings of 125 GeV Higgs in NP models with SM particles (in units of the corresponding SM couplings). In the conventional $U(1)_X$ model, we have

$$\begin{aligned}C_{h_{125}uu} &= C_{h_{25}uu} = Z_{h,12} + Z_{h,22}\kappa_1, \quad C_{h_{125}dd} = C_{h_{25}dd} = Z_{h,12} + Z_{h,22}\kappa_2, \\ C_{h_{125}ee} &= C_{h_{25}dd} = Z_{h,12}, \quad C_{h_{125}VV} = C_{h_{25}VV} = Z_{h,12}.\end{aligned}\quad (24)$$

III. NUMERICAL RESULTS

Assuming the mass of the lightest Higgs boson to be approximately 95 GeV and the next-to-lightest Higgs boson corresponds to the measured SM-like Higgs [52] with the mass given by

$$m_h = 125.09 \pm 0.24 \text{ GeV}, \quad (25)$$

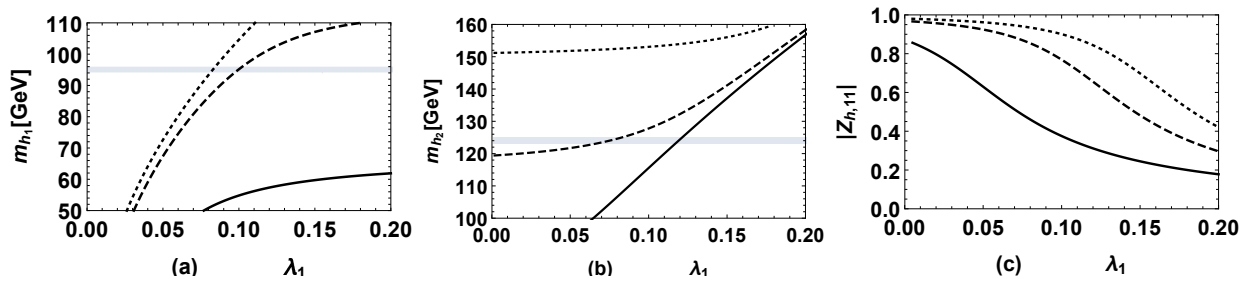


FIG. 1: Taking $\Lambda = 15$ TeV, $\lambda_4 = 0.001$, the mass of the lightest Higgs m_{h_1} versus λ_1 is plotted in (a), the mass of the next-to-lightest Higgs versus λ_1 is plotted in (b), and the Higgs mixing parameter $|Z_{h,11}|$ versus λ_4 is plotted in (c). The solid, dashed, dotted lines denote the results for $\lambda_2 = 0.00001, 0.00003, 0.00005$ respectively, the gray areas denote the range $94 \text{ GeV} < m_{h_1} < 96 \text{ GeV}$ for (a) and $124 \text{ GeV} < m_{h_2} < 126 \text{ GeV}$ for (b).

we present the numerical results for the signal strengths of diphoton and ditau processes in this section. The outcomes of the process are primarily influenced by parameters λ_1 , λ_2 , λ_4 , Λ , κ_1 and κ_2 . Here, λ_1 , λ_2 , λ_4 are constants in the scalar sectors. Λ is the vacuum expectation value scalar S_2 , and it is constrained by data from FCNC and particle colliders, necessitating it to be larger than 14.14 TeV [42] which can be released under the minimal flavor violation assumption above.

Firstly, we investigate the masses of the lightest and next-to-lightest Higgs bosons within the model. Taking $\Lambda = 15$ TeV and $\lambda_4 = 0.001$, we plot the mass of the lightest Higgs m_{h_1} versus λ_1 in Fig. 1 (a), the mass of the next-to-lightest Higgs m_{h_2} versus λ_1 in Fig. 1 (b), and the Higgs mixing parameter $|Z_{h,11}|$ versus λ_4 in Fig. 1 (c), where the solid, dashed, dotted lines denote the results for $\lambda_2 = 0.00001, 0.00003, 0.00005$ respectively. The gray areas denote the range $94 \text{ GeV} < m_{h_1} < 96 \text{ GeV}$ for Fig. 1 (a) and $124 \text{ GeV} < m_{h_2} < 126 \text{ GeV}$ for Fig. 1 (b). It can be observed from the plot that λ_1 and λ_2 significantly influence the masses of the two light Higgs bosons, and both m_{h_1} and m_{h_2} increase as λ_1 increases. Notably, both the 95 GeV Higgs and the SM-like Higgs with a mass of 125 GeV are attainable within the model. Fig. 1 (a) shows that λ_2 is constrained around 0.00003 with λ_1 slightly less than 0.1 for $m_{h_1} \approx 95 \text{ GeV}$ and $m_{h_2} \approx 125 \text{ GeV}$ in our chosen parameter space. λ_1 , λ_2 and λ_4

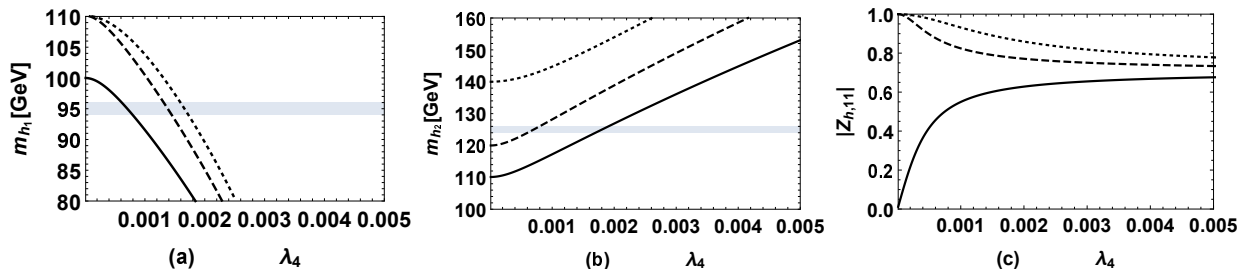


FIG. 2: Taking $\lambda_1 = 0.1$, $\lambda_2 = 0.00005$, the mass of the lightest Higgs m_{h_1} versus λ_4 is plotted in (a), the mass of the next-to-lightest Higgs m_{h_2} versus λ_4 is plotted in (b), and the Higgs mixing parameter $|Z_{h,11}|$ versus λ_4 is plotted in (c). The solid, dashed, dotted lines denote the results for $\Lambda = 10, 12, 14$ TeV respectively, the gray areas denote the range $94 \text{ GeV} < m_{h_1} < 96 \text{ GeV}$ for (a) and $124 \text{ GeV} < m_{h_2} < 126 \text{ GeV}$ for (b).

collectively determine the two light Higgs masses.

Setting $\lambda_1 = 0.1$, $\lambda_2 = 0.00005$, we plot m_{h_1} , m_{h_2} and the Higgs mixing parameter $|Z_{h,11}|$ versus λ_4 in Fig. 2 (a), (b), (c) respectively, where the solid, dashed, dotted lines denote the results for $\Lambda = 10, 12, 14$ TeV respectively. The gray areas denote the range $94 \text{ GeV} < m_{h_1} < 96 \text{ GeV}$ for Fig. 2 (a) and $124 \text{ GeV} < m_{h_2} < 126 \text{ GeV}$ for Fig. 2 (b). It can be observed from Fig. 2 that m_{h_1} increases with the increasing of λ_4 , while m_{h_2} decreases with the increasing of λ_4 . Both m_{h_1} and m_{h_2} increase as Λ increasing. Fig. 2 shows that in our chosen parameter space, λ_4 is around 0.00002 when $m_{h_1} \approx 95 \text{ GeV}$ and $m_{h_2} \approx 125 \text{ GeV}$.

Based on the preceding analysis, it is evident that both the 95 GeV lightest Higgs boson and the 125 GeV SM-like Higgs boson are attainable in the model, and $\lambda_1, \lambda_2, \lambda_4, \Lambda$ collectively determine the two light Higgs masses. Subsequently, we investigate the potential of the 95 GeV Higgs boson within the flavor-dependent $U_1(x)$ model to account for the observed excesses in diphoton and ditau events. To comprehensively understand the collective influences of $\lambda_1, \lambda_2, \lambda_4, \Lambda, \kappa_1$ and κ_2 on the signal strength of diphoton and ditau events, we scan the following parameter space

$$\lambda_1 = (0.0001, 0.2), \Lambda = (14, 20) \text{ TeV}, \kappa_1 = (0.0001, 1), \kappa_2 = (0.0001, 1), \quad (26)$$

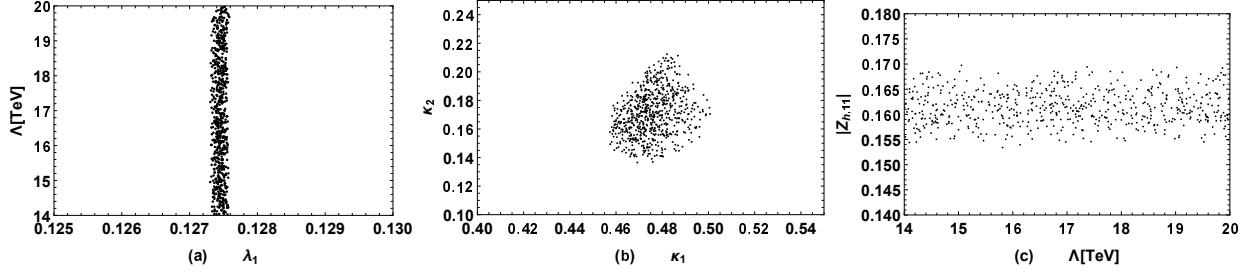


FIG. 3: Keeping $m_{h_1} = 95$ GeV, $m_{h_2} = 125$ GeV, the measured 125 GeV Higgs signals in the range shown in Eq. (28), $0.21 < \mu(h_{95})_{\gamma\gamma} < 0.52$, $0.7 < \mu(h_{95})_{\tau\tau} < 1.7$, and scanning the parameter space in Eq. (26), the allowed ranges of $\lambda_1 - \Lambda$ (a), $\kappa_1 - \kappa_2$ (b) are plotted. In the allowed ranges shown in (a) and (b), the Higgs mixing parameter $|Z_{h,11}|$ versus Λ is plotted in (c).

where λ_2, λ_4 are determined by

$$\lambda_2 = \frac{(m_{h_1}^2 + m_{h_2}^2 - 2\lambda_1 v^2)}{2\Lambda^2}, \quad \lambda_4 = \frac{\sqrt{(m_{h_1}^2 - 2\lambda_1 v^2)(2\lambda_1 v^2 - m_{h_2}^2)}}{v \Lambda}, \quad (27)$$

with $m_{h_1} = 95$ GeV and $m_{h_2} = 125$ GeV. Keeping the measured 125 GeV Higgs signals in the range [52]

$$\begin{aligned} \mu_{WW^*} &= 1.00 \pm 0.08, \quad \mu_{ZZ^*} = 1.02 \pm 0.08, \quad \mu_{\gamma\gamma^*} = 1.10 \pm 0.07, \\ \mu_{c\bar{c}} &= 8 \pm 22, \quad \mu_{b\bar{b}} = 0.99 \pm 0.12, \quad \mu_{\mu\bar{\mu}} = 1.21 \pm 0.35, \quad \mu_{\tau\bar{\tau}} = 0.99 \pm 0.12, \end{aligned} \quad (28)$$

and the two CMS excesses at about 95 GeV in the ranges $0.21 < \mu(h_{95})_{\gamma\gamma} < 0.52$, $0.7 < \mu(h_{95})_{\tau\tau} < 1.7$, we plot the allowed ranges of $\lambda_1 - \Lambda$, $\kappa_1 - \kappa_2$ in Fig. 3 (a), Fig. 3 (b) respectively. In the allowed ranges shown in Fig. 3 (a) and Fig. 3 (b), the Higgs mixing parameter $|Z_{h,11}|$ versus Λ is plotted in Fig. 3 (c).

It is obvious from Fig. 3 that the flavor-dependent $U(1)_X$ model can account well for both the diphoton and ditau excesses at about 95 GeV. Fig. 3 (a) shows that the parameter Λ is not strictly limited by the diphoton and ditau excesses, while λ_1 is strictly limited. Because Λ affects the 95 GeV Higgs signals and 125 GeV Higgs signals mainly through the mixing effects of S_1 and S_2 as shown in Eq. (13). It is obvious that the dependence of A on Λ by the terms $\lambda_4 \Lambda$ and $\lambda_2 \Lambda^2$, and both the two terms depend on λ_1 for fixed m_{h_1} ,

m_{h_2} as shown in Eq. (27). Hence, the excesses are satisfied quite independent of the value of Λ , while λ_1 is strictly limited. In addition, Eq. (12) shows that the SM-like Higgs mass m_{h_2} mainly depends on λ_1 which also leads to the strict constraint on λ_1 . κ_1 and κ_2 are also limited strictly as shown in Fig. 3 (b), by all the constrains taken into consideration. The diphoton and ditau excesses at about 95 GeV prefer the ranges $0.128 \gtrsim \lambda_1 \gtrsim 0.127$, $0.52 \gtrsim \kappa_1 \gtrsim 0.45$ and $0.22 \gtrsim \kappa_2 \gtrsim 0.12$. Fig. 3 (c) shows that $|Z_{h,11}|$ is located in the range $0.15 \lesssim |Z_{h,11}| \lesssim 0.17$, because the 95 GeV state is dominated by the extra singlet scalar in the model and the Higgs squared mass matrix in Eq. (10) is written on the basis (S_1, S_2, S_3) . Finally, provided that the excesses persist, the precision measurement of the 125 GeV Higgs couplings has potential to detect this scenario, because the introducing of a light Higgs boson below 125 GeV changes the coupling properties of 125 GeV Higgs.

IV. SUMMARY

Considering the diphoton and ditau excesses at a mass about 95 GeV in the CMS data, we focus on explaining these two excesses in flavor-dependent $U(1)_X$ model, because the model can produce a 95 GeV light Higgs naturally by introducing the specific singlet state. And this new scalar state interacts with the quark sector directly to explain the flavor numbers of the fermion sector, which provides great potential to explain the two excesses. Considering the specific Higgs state as the lightest Higgs boson, it is found that the specific parameters $\lambda_1, \lambda_2, \lambda_4$ and Λ in the model affects the theoretical predictions on the two light Higgs boson masses significantly. Taking the lightest Higgs boson mass at about 95 GeV and the next-to-lightest Higgs boson mass at about 125 GeV, the numerical results show that the specific Higgs state in flavor-dependent $U(1)_X$ model can account for the observed CMS diphoton and ditau excesses at about 95 GeV well. In addition, fitting $\mu(h_{95})_{\gamma\gamma}, \mu(h_{95})_{\tau\tau}$ in the CMS 1σ interval will impose stringent constraints on the parameter space of the flavor-dependent $U(1)_X$ model, and the fact can be seen explicitly in Fig. 3.

Acknowledgments

The work has been supported by the National Natural Science Foundation of China (NNSFC) with Grants No. 12075074, No. 12235008, Hebei Natural Science Foundation for Distinguished Young Scholars with Grant No. A2022201017, Natural Science Foundation of Guangxi Autonomous Region with Grant No. 2022GXNSFDA035068, and the youth top-notch talent support program of the Hebei Province.

- [1] S. Chatrchyan *et al.* [CMS], Phys. Lett. B **716**, 30-61 (2012).
- [2] G. Aad *et al.* [ATLAS], Phys. Lett. B **716**, 1-29 (2012).
- [3] A. Tumasyan *et al.* [CMS], Nature **607**, no.7917, 60-68 (2022).
- [4] [ATLAS], Nature **607**, no.7917, 52-59 (2022) [erratum: Nature **612**, no.7941, E24 (2022)].
- [5] [CMS], CMS-PAS-HIG-14-037.
- [6] A. M. Sirunyan *et al.* [CMS], Phys. Lett. B **793**, 320-347 (2019).
- [7] C. Arcangeletti. on behalf of ATLAS collaboration, LHC Seminar, 7th of June, 2023.
- [8] [ATLAS], ATLAS-CONF-2018-025.
- [9] A. Tumasyan *et al.* [CMS], JHEP **07**, 073 (2023).
- [10] S. Gascon-Shotkin, CMS, Talk at MoriondEW: Searches for additional Higgs bosons at low mass, 2023.
- [11] S. Moretti and S. Munir, Eur. Phys. J. C **47**, 791-803 (2006).
- [12] U. Ellwanger, Phys. Lett. B **698**, 293-296 (2011).
- [13] J. Cao, Z. Heng, T. Liu and J. M. Yang, Phys. Lett. B **703**, 462-468 (2011).
- [14] D. Albornoz Vasquez, G. Belanger, C. Boehm, J. Da Silva, P. Richardson and C. Wymant, Phys. Rev. D **86**, 035023 (2012).
- [15] U. Ellwanger and C. Hugonie, Adv. High Energy Phys. **2012**, 625389 (2012).
- [16] F. Boudjema and G. D. La Rochelle, Phys. Rev. D **86**, 115007 (2012).
- [17] K. Schmidt-Hoberg and F. Staub, JHEP **10**, 195 (2012).
- [18] M. Badziak, M. Olechowski and S. Pokorski, JHEP **06**, 043 (2013).

- [19] M. Badziak, M. Olechowski and S. Pokorski, PoS **EPS-HEP2013**, 257 (2013).
- [20] R. Barbieri, D. Buttazzo, K. Kannike, F. Sala and A. Tesi, Phys. Rev. D **88**, 055011 (2013).
- [21] J. W. Fan, J. Q. Tao, Y. Q. Shen, G. M. Chen, H. S. Chen, S. Gascon-Shotkin, M. Lethuillier, L. Sgandurra and P. Soulet, Chin. Phys. C **38**, 073101 (2014).
- [22] C. T. Potter, Eur. Phys. J. C **76**, no.1, 44 (2016).
- [23] U. Ellwanger and M. Rodriguez-Vazquez, JHEP **02**, 096 (2016).
- [24] J. Cao, X. Guo, Y. He, P. Wu and Y. Zhang, Phys. Rev. D **95**, no.11, 116001 (2017).
- [25] J. Cao, X. Jia, Y. Yue, H. Zhou and P. Zhu, Phys. Rev. D **101**, no.5, 055008 (2020).
- [26] T. Biekötter, M. Chakraborti and S. Heinemeyer, Eur. Phys. J. C **80**, no.1, 2 (2020).
- [27] T. Biekötter and M. O. Olea-Romacho, JHEP **10**, 215 (2021).
- [28] T. Biekötter, A. Grohsjean, S. Heinemeyer, C. Schwanenberger and G. Weiglein, Eur. Phys. J. C **82**, no.2, 178 (2022).
- [29] S. Heinemeyer, C. Li, F. Lika, G. Moortgat-Pick and S. Paasch, Phys. Rev. D **106**, no.7, 075003 (2022).
- [30] T. Biekötter, S. Heinemeyer and G. Weiglein, JHEP **08**, 201 (2022).
- [31] T. Biekötter, S. Heinemeyer and G. Weiglein, Eur. Phys. J. C **83**, no.5, 450 (2023).
- [32] T. Biekötter, S. Heinemeyer and G. Weiglein, [arXiv:2303.12018 [hep-ph]].
- [33] D. Azevedo, T. Biekötter and P. M. Ferreira, [arXiv:2305.19716 [hep-ph]].
- [34] J. A. Aguilar-Saavedra, H. B. Câmara, F. R. Joaquim and J. F. Seabra, [arXiv:2307.03768 [hep-ph]].
- [35] D. Sachdeva and S. Sadhukhan, Phys. Rev. D **101**, no.5, 055045 (2020).
- [36] T. Biekötter, S. Heinemeyer and C. Muñoz, Eur. Phys. J. C **78**, no.6, 504 (2018).
- [37] T. Biekötter, S. Heinemeyer and C. Muñoz, Eur. Phys. J. C **79**, no.8, 667 (2019).
- [38] R. Barate *et al.* [LEP Working Group for Higgs boson searches, ALEPH, DELPHI, L3 and OPAL], Phys. Lett. B **565**, 61-75 (2003).
- [39] S. Ashanujjaman, S. Banik, G. Coloretti, A. Crivellin, B. Mellado and A. T. Mulaudzi, [arXiv:2306.15722 [hep-ph]].
- [40] A. Azatov, R. Contino and J. Galloway, JHEP **04**, 127 (2012).
- [41] S. Heinemeyer and T. Stefaniak, PoS **CHARGED2018**, 016 (2019).

- [42] D. Van Loi and P. Van Dong, Eur. Phys. J. C **83**, no.11, 1048 (2023).
- [43] [CMS], CMS-PAS-EXO-21-018.
- [44] S. Iguro, T. Kitahara and Y. Omura, Eur. Phys. J. C **82**, no.11, 1053 (2022).
- [45] R. S. Chivukula and H. Georgi, Phys. Lett. B **188**, 99-104 (1987).
- [46] L. J. Hall and L. Randall, Phys. Rev. Lett. **65**, 2939-2942 (1990).
- [47] A. J. Buras, P. Gambino, M. Gorbahn, S. Jager and L. Silvestrini, Phys. Lett. B **500**, 161-167 (2001).
- [48] G. D'Ambrosio, G. F. Giudice, G. Isidori and A. Strumia, Nucl. Phys. B **645**, 155-187 (2002).
- [49] G. Isidori, Y. Nir and G. Perez, Ann. Rev. Nucl. Part. Sci. **60**, 355 (2010).
- [50] A. Djouadi, J. Kalinowski and M. Spira, Comput. Phys. Commun. **108**, 56-74 (1998).
- [51] A. Arbey, A. Deandrea, F. Mahmoudi, and A. Tarhini, Anomaly mediated supersymmetric models and Higgs data from the LHC, Phys. Rev. D **87**, 115020 (2013), arXiv:1304.0381 [hep-ph].
- [52] R. L. Workman *et al.* [Particle Data Group], PTEP **2022**, 083C01 (2022).